# Dynamics of a trapped two-level and three-level atom interacting with classical electromagnetic field

Aditi Ray
*Theoretical Physics Division, Bhabha Atomic Research Centre, Mumbai-400085, India*
(Received 21 August 2002; published 10 March 2004)

The dynamics of a two-level atom driven by a single laser beam and three-level atom (Lambda configuration) irradiated by two laser beams are studied taking into account of the quantized center-of-mass motion of the atom. It is shown that the trapped atom system under appropriate resonance condition exhibits the large time-scale revivals when the index of the vibrational sideband responsible for the atomic electronic transition is greater than unity. The revival times are shown to be dependent on the initial number of vibrational excitations and the magnitude of the Lamb-Dicke parameter. The sub-Poissonian statistics in vibrational quantum number is observed at certain time intervals. The minimum time of interaction for which the squeezed states of motional quadrature are generated is found to be decreasing with the increase in the Lamb-Dicke parameter.

DOI: 10.1103/PhysRevA.69.033806 PACS number(s): 42.50.Ct, 42.50.Vk

## I. INTRODUCTION

During the last decade a significant progress has been made in the experimental and theoretical methods of laser cooling of the free as well as the trapped two-level and three-level atoms. With the various cooling techniques, namely the Doppler cooling [1], sideband cooling [1], Sisyphus cooling [2], dark-state cooling [3], and so on, the temperature of the atoms can be lowered to such a limit that they start behaving like the quantum-mechanical objects. The methods of preparing such a trapped atom in a chosen quantum state of its center-of-mass (c.m.) motion, such as Fock state, coherent state, squeezed state, the Schrödinger cat states, are already accomplished [4]. The generation of these nonclassical states have found their application in the field of quantum computation.

The nonlinear and the quantum effects of the interactions involving one atom with few energy levels and one or more near resonant electromagnetic (em) fields are generally studied either by quantizing the interacting field or by allowing the atom to undergo quantized motion around its c.m. by placing it in a harmonic trap. The effects arising due to the first method have been investigated extensively theoretically as well as experimentally, whereas not enough study is made in the effects due to the quantization of the atomic motion. This paper is an attempt to throw some light on the dynamical and the statistical properties of such system. The dynamics of the atomic inversion of a two-level trapped atom have been studied for initial coherent vibration of the atomic c.m. [5]. The nonlinear effects arising due to the interaction of a single three-level atom with Raman lasers have been analyzed to generate the squeezed states at short interaction times [6]. The wave-mixing response of a two-level atom in a harmonic trap interacting with a classical em field has been studied and it has been shown that the quantized motion of the trapped atom can significantly influence the nonlinear optical processes such as multiwave mixing [7].

In this paper we study dynamics of an atomic system embedded in a harmonic trap and interacting with classical em fields paying particular attention to the revival times. We also find the system parameters that are responsible for the occurrence of the large time-scale revivals. The model cases chosen for studying the above phenomena are (i) a single two-level atom undergoing quantized motion around its c.m. and irradiated by a monochromatic field and (ii) a single three-level atom undergoing quantized motion and Raman coupled with two laser fields. Vogel and de Matos Filho [5] have shown that under appropriate resonance conditions and far from the Lamb-Dicke (LD) regime the interaction of such a trapped two-level atom with classical em field is well described by a Hamiltonian which is similar to that nonlinearly coupled multiquantum Jaynes-Cummings (JC) model. By adiabatic elimination of the second excited state, which is assumed to be far-off resonance, we have reduced the three-level atom in Raman ($\Lambda$) configuration to an *effective two-level model*. We also show that far from the LD regime this effective two-level atom Hamiltonian can be reduced to a form that is equivalent to the one derived in the case of trapped two-level atom interacting with a single classical field.

The present paper investigates the collapse and revival properties of trapped atom system for the above described model cases. It will be shown that, if the frequency (relative frequency) of the interacting classical field(s) is resonant with the $n$th vibrational sideband, then the dynamical variables exhibit large time-scale revivals or "delayed revivals," when $n$ is greater than unity. In order to provide an estimate for the time for which this delayed revival occurs, we derive the general expression for the revival time for model I when the interacting field is detuned to any $n$th motional sideband. It is shown that, in both the models, the ratio of the revival times for the second and the first sideband transition is inversely proportional to the square root of the average number of the vibrational excitation for the initial coherent vibration. For model I this ratio is inversely proportional to the LD parameter. In the case of model II this time ratio is a complicated function of the LD parameters of both the fields. We discuss the special cases of model II when the ratio of the

 

revival times for second and first sideband transition processes becomes same as that of model I.

The long time-scale revivals discussed in this paper are not the same as the *super-revivals* that are studied by Dutra *et al.* [8] in cavity QED system and by Moya-Cess *et al.* [9] in trapped atom system. The authors of Ref. [9] have demonstrated the existence of the super-revivals in trapped three-level atom system beyond the LD regime. The large time-scale revivals studied here, which we call delayed revivals, are normal revivals occurring at late times due to some change in system preparation, whereas the super-revivals are the revival of revivals occurring at larger times. Our study suggests that the delayed-revival phenomena may be observed within and beyond the LD regime.

The difference between the nonlinear multiquantum JC model for the cavity field and that of the trapped atom system is that the effective interaction in the latter case corresponds to the resultant process of all the finite quantum JC-type interactions starting with zero vibrational quantum. This inherent nonlinearity in the coupling of the atomic electronic and motional degrees of freedom leads to very interesting and distinct nonclassical phenomena. This paper investigates the possible generation of the nonclassical states of the vibrational modes by examining the second-order coherence function. It is shown that at certain times of interaction the second-order coherence function is less than unity thereby implying that the normally ordered variance of the vibrational excitation is less than zero. At those times the vibrational modes are said to follow sub-Poissonian statistics, an effect similar to the antibunching of the photons in the case of cavity modes coupled with the atomic electronic states.

Finally, we show that at certain time intervals of interaction the variance in either component of the motional (vibrational) quadrature is less than the corresponding coherent state value, thereby generating the squeezed motional state for that quadrature. It is also found that the early onset to the quadrature squeezing is achieved by increasing the value of the LD parameter.

The organization of the paper is as follows. In Sec. II we describe the two-level atom under consideration and the model Hamiltonian. Sec. III describes the model system of three-level atom in the harmonic trap and presents the effective two-level atom Hamiltonian. In Sec. IV we evaluate the wave function at any later time assuming that the atom is in the ground state initially, undergoing coherent vibrations around its center of mass. In Sec. V we study the dynamics of the atomic inversion for the two models. Here we derive the expression for revival time for *n*th sideband transition process. The time for which the revival occurs first in model I and model II is compared for a particular sideband transition. Section VI shows the collapse and revival pattern of the vibrational quantum number for the two models. In Sec. VII we study the generation of the nonclassical states of the vibrational mode by investigating the appearance of sub-Poissonian statistics of the average excitation number. Finally, in Sec. VIII the squeezing properties of the motional quadratures are discussed. The conclusions are summed up in Sec. IX. The details of the adiabatic removal of the far resonant excited state to reduce the three-level atom Hamiltonian to the effective two-level Hamiltonian are provided in the Appendix.

## II. MODEL I: TWO-LEVEL ATOM

In this section we depict the model of the two-level atom trapped in a harmonic potential and irradiated by a standing wave field. The system under consideration consists of a two-level atom of transition frequency $\omega_0$ in a harmonic trap. Let the frequency of oscillation of the atom in the trap be $\nu$. We assume that the atom is interacting with a classical em field of frequency $\omega_l$ directed along one of the principal axes of the harmonic potential so that the motion of the atom is restricted to one dimension only. If the field is resonant with *n*th red sideband, i.e., if

$$\omega_l = \omega_0 - n\nu, \tag{1}$$

then the Hamiltonian describing the coupling between the atomic internal and external degrees of freedom in rotating wave approximation (RWA) and beyond the LD limit is given by ($\hbar = 1$) [5,10]

$$H = \nu a^\dagger a + \omega_0 \sigma_z + \epsilon \sum_{k=0}^{\infty} [f_k (a^\dagger)^k a^{k+n} \sigma_+ e^{-i\omega_l t} + \text{H.c.}], \tag{2}$$

where $\epsilon$ is the atom-field coupling constant and $a$ and $a^\dagger$ are the annihilation and the creation operators for the vibrational quantum. The atomic raising and lowering operators are denoted by $\sigma_+$ and $\sigma_-$, respectively. The LD parameter-dependent constant $f_k$ has the following form,

$$f_k = \frac{(-1)^k \xi^{2k+n} \exp(-\xi^2/2)}{k!\,(k+n)!} \sin\left(\frac{n\pi}{2} + \phi_0\right). \tag{3}$$

Here $\xi$ is the LD parameter and $\phi_0$ defines the equilibrium position of the atom in the trap with respect to the field. The RWA assumes that the separation $\nu$ between the sidebands is larger than the Rabi frequency of transition between the atomic electronic levels. This puts an upper bound on the value of the applied field strength. Now, in a frame rotating with $\omega_l$, the Hamiltonian (2) reads as

$$H_I = \nu a^\dagger a + n\nu \sigma_z + \epsilon \sum_{k=0}^{\infty} [f_k (a^\dagger)^k a^{k+n} \sigma_+ + \text{H.c.}]. \tag{4}$$

We will use the Hamiltonian (4) to study the dynamical and statistical properties of this system.

## III. MODEL II: THREE-LEVEL ATOM IN A $\Lambda$ CONFIGURATION

In this section we describe the model for the three-level trapped atom and derive its effective two-level Hamiltonian. The scheme for the adiabatic elimination of a level of cavity QED has been successfully adopted in the trapped atom case.

We consider a single three-level atom in Raman configuration ($\Lambda$ type) trapped in a harmonic potential and interacting with two lasers of frequencies $\omega_1$ and $\omega_2$ with $\xi_1$ and $\xi_2$ as the corresponding LD parameters. Both the fields are treated classically. The fields are assumed to be propagating along one of the principal axes of the harmonic potential so that we have one-dimensional problem. The energy-level diagram for a trapped three-level atom in a $\Lambda$ configuration

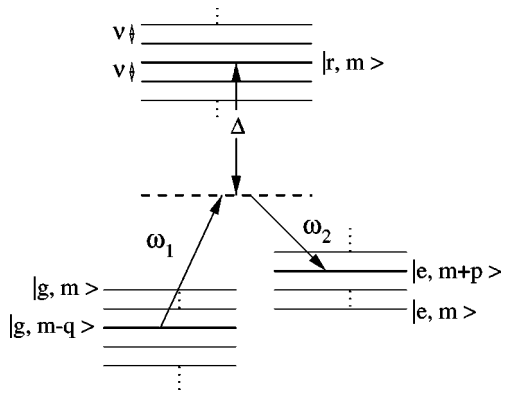


FIG. 1. The energy-level diagram of the trapped three-level atom in Λ configuration.

is shown in Fig. 1. It is the generalization of the electronic Λ scheme in trapped atom system with the levels $|g,m-q\rangle$ and $|e,m+p\rangle$ being independently coupled with the level $|r,m\rangle$. The notations $|g,m-q\rangle \equiv |g\rangle|m-q\rangle$, $|e,m+p\rangle \equiv |e\rangle|m+p\rangle$, and $|r,m\rangle \equiv |r\rangle|m\rangle$ represent the vibrational-assisted electronic states where $|g\rangle$, $|e\rangle$, and $|r\rangle$ denote the bare electronic states of the three-level atom with the corresponding energies $E_g$, $E_e$, and $E_r$, respectively, and $|m-q\rangle$, $|m+p\rangle$, and $|m\rangle$ are the Fock states of the harmonic trap. We have also assumed that the field frequency $\omega_1$ is resonant with the $q$th red-shifted sideband whereas the field frequency $\omega_2$ is resonant with the $p$th blue-shifted sideband of the vibrational states. The system is tuned consistent with two-photon energy conservation so that the detuning $\Delta$ satisfies the relations

$$\omega_1 + \Delta = E_r - E_g - q\nu,$$
$$\omega_2 + \Delta = E_r - E_e + p\nu, \tag{5}$$

where $\nu$ is the frequency of oscillation of the atomic c.m. in the trap. From Eq. (5) we get the relative frequency $\omega_l$ of the two fields as

$$\omega_l = \omega_1 - \omega_2 = \omega_0 - n\nu, \quad n = p + q, \tag{6}$$

where $\omega_0 = E_e - E_g$ is the effective transition frequency between the levels $|e\rangle$ and $|g\rangle$. Equation (6) implies that the relative frequency of the two laser beams is resonant with the $n$th red-shifted vibrational sideband. Note that the resonance condition (6) is equivalent to Eq. (1) of Sec. II.

Next, we assume that the detuning $\Delta$ is sufficiently large such that $\Delta \gg E_e - E_g$. Under this assumption we will show that the laser fields effectively drive the electric-dipole forbidden transition $|g\rangle \leftrightarrow |e\rangle$. The interaction of the trapped atom with the standing-wave field is governed by the total Hamiltonian

$$H = E_g\sigma_{gg} + E_r\sigma_{rr} + E_e\sigma_{ee} + \nu a^\dagger a + \epsilon_1 \sin(k_1 R + \phi_1)(\sigma_{rg}e^{-i\omega_1 t} + \text{H.c.}) + \epsilon_2 \sin(k_2 R + \phi_2)(\sigma_{re}e^{-i\omega_2 t} + \text{H.c.}), \tag{7}$$

where $\phi_i = k_i R_0 (i = 1,2)$ are the phases introduced due to equilibrium position of the atom in the trap with respect to the nodes and the antinodes of the interacting fields of frequencies $\omega_i (i = 1,2)$. The operators $\sigma_{ij}(i,j = g,e,r)$ are the atomic transition operators.

Now, the adiabatic removal of the level $|r\rangle$ and introduction of the creation and annihilation operators of the motional states $a^\dagger$, $a$ in the "sine" terms, as described in the Appendix, results in the effective interaction Hamiltonian given by

$$H_I = n\nu\sigma_z + \nu a^\dagger a + \frac{\epsilon_r}{2}\{e^{i\xi_+(a+a^\dagger)}\, e^{i\phi_+} + e^{-i\xi_+(a+a^\dagger)}\, e^{-i\phi_+} - e^{i\xi_-(a+a^\dagger)}\, e^{i\phi_-} - e^{-i\xi_-(a+a^\dagger)}e^{-i\phi_-}\}\{\sigma_+ + \sigma_-\}, \tag{8}$$

where $\epsilon_r$ is the effective coupling constant of the two-level representation of the three-level atom system. In the following we will analyze the Hamiltonian (8) in the LD regime as well as far from the LD regime of both the fields.

### A. Hamiltonian in the LD regime

In this case we have $\xi_1 \ll 1$ and $\xi_2 \ll 1$. We examine the Hamiltonian (8) in some special cases.

*Case I.* $\xi_2 \ll \xi_1$, so $\xi_+ = \xi_- \approx \xi_1$. Since both $\xi_+$ and $\xi_-$ are very much less than unity hence we can retain the terms upto the first order in $\xi_1$ in the exponentials appearing in Eq. (8) and write the total Hamiltonian as

$$H_I = n\nu\sigma_z + \nu a^\dagger a + \frac{\epsilon_r}{2}\{[1 + i\xi_1(a + a^\dagger)]e^{i\phi_+} + [1 - i\xi_1(a + a^\dagger)]e^{-i\phi_+} - [1 + i\xi_1(a + a^\dagger)]e^{i\phi_-} - [1 - i\xi_1(a + a^\dagger)]e^{-i\phi_-}\}\{\sigma_+ + \sigma_-\}, \tag{9}$$

which can be further simplified to

$$H_I = n\nu\sigma_z + \nu a^\dagger a + \epsilon_r[(\cos\phi_+ - \cos\phi_-) - \xi_1(a + a^\dagger)(\sin\phi_+ - \sin\phi_-)]\{\sigma_+ + \sigma_-\}. \tag{10}$$

For appropriate choices of the equilibrium positions of the atomic c.m. with respect to the fields and in RWA one can rewrite Eq. (10) in a form that is analogous to usual single-photon JC Hamiltonian.

Verify that, if $\phi_1 = \pi$ and $\phi_2 = \pi/6$ or $\phi_1 = 0$ and $\phi_2 = 7\pi/6$, then in RWA Eq. (10) reduces to

$$H_I = n\nu\sigma_z + \nu a^\dagger a + \epsilon_r\xi_1(a^\dagger\sigma_- + \sigma_+ a). \tag{11}$$

*Case II.* $\xi_1 = \xi_2$, so $\xi_+ = 2\xi_1$ and $\xi_- = 0$. Hence, in the LD regime ($\xi_+ \ll 1$) the Hamiltonian (8) reduces to

$$H = n\nu\sigma_z + \nu a^\dagger a + \epsilon_r[(\cos\phi_+ - \cos\phi_-) - 2\xi_1(a + a^\dagger)\sin\phi_+] \times\{\sigma_+ + \sigma_-\}. \tag{12}$$

Note that, for $\phi_1 = 0$ and $\phi_2 = 7\pi/6$ or $\phi_1 = 7\pi/6$ and $\phi_2 = 0$ and in RWA, Eq. (12) reduces to Eq. (11). Thus in both the above cases the interaction is governed by a Hamiltonian that one would expect in the case of model I in the LD regime with $\xi_1$ as the LD parameter.

### B. Hamiltonian beyond the LD regime

By disentangling the exponentials containing $a, a^\dagger$ we may write the Hamiltonian (8) as

$$H_I = n\nu\sigma_z + \nu a^\dagger a + \frac{\epsilon_r}{2}\Bigg[ e^{-\xi_+^2/2}\Bigg\{ \sum_{k,l} \frac{(i\xi_+)^{k+l}}{k!\,l!}(a^\dagger)^k a^l e^{i\phi_+} + \sum_{k,l} \frac{(-i\xi_+)^{k+l}}{k!\,l!}(a^\dagger)^k a^l e^{-i\phi_+}\Bigg\} - e^{-\xi_-^2/2}\Bigg\{ \sum_{k,l} \frac{(i\xi_-)^{k+l}}{k!\,l!}(a^\dagger)^k a^l e^{i\phi_-} + \sum_{k,l} \frac{(-i\xi_-)^{k+l}}{k!\,l!}(a^\dagger)^k a^l e^{-i\phi_-}\Bigg\}\Bigg]\{\sigma_+ + \sigma_-\}. \tag{13}$$

For the field frequencies close to the lower motional sideband resonance, i.e.,

$$|\omega_l - (\omega_0 - n\nu)| \ll n\nu,$$

only transitions with decreasing quantum number by $n$ are important. Under the above resonance condition along with the assumption that only one transition can take place at one time the Hamiltonian (13), in a frame rotating with $\omega_l$ and in RWA, assumes the following form of nonlinear multiquantum JC interaction

$$H_I = n\nu\sigma_z + \nu a^\dagger a + \epsilon_r\Bigg[\sum_{k=0}^{\infty} F_k (a^\dagger)^k a^{k+n}\sigma_+ + F_k^*(a^\dagger)^{k+n}a^k\sigma_-\Bigg], \tag{14}$$

where the parameter

$$F_k = P_k - Q_k \tag{15}$$

is a function of the LD parameters of both the fields and the equilibrium positions of the atom, with

$$P_k = e^{-\xi_+^2/2}\frac{(-1)^k(\xi_+)^{2k+n}}{k!\,(k+n)!}\cos\left(\frac{n\pi}{2} + \phi_+\right) \tag{16}$$

and

$$Q_k = e^{-\xi_-^2/2}\frac{(-1)^k(\xi_-)^{2k+n}}{k!\,(k+n)!}\cos\left(\frac{n\pi}{2} + \phi_-\right). \tag{17}$$

The Hamiltonian (14) is equivalent to the Hamiltonian (4) of Sec. II with $f_k$ being replaced by $F_k$.

We have thus shown that the three-level atom undergoing quantized motion in a harmonic trap and interacting with two classical fields can be reduced to an effective two-level atom in both the LD regime as well as beyond that regime. This is, to our knowledge, the first attempt towards the adoption of the scheme of adiabatic elimination of a level to reduce the three-level trapped atom to the effective two-level picture in the most general form.

The Hamiltonian (14) has some special properties. If one of the driving fields is turned off (the LD parameter corresponding to that field vanishes) then it is straightforward to show that $P_k = Q_k$ and $F_k = 0$, hence the coupling between the atomic electronic and motional states breaks. Further, if the LD parameters of both the fields are equal then $Q_k$ vanishes and $F_k$ reduces to $P_k$. In this case the system behaves like a two-level atom driven by single em field with $2\xi$ as the LD parameter.

We will use Eq. (14) to the study of the dynamics of model II.

## IV. TIME EVOLUTION OF WAVE FUNCTION

In the last two sections we have presented the Hamiltonians for model I [Eq. (4)] and model II [Eq. (14)]. The eigenstates of both the Hamiltonians have the general form

$$|\psi_m^\pm\rangle = \frac{1}{\sqrt{2}}[|m,e\rangle \pm |m+n,g\rangle], \tag{18}$$

where $|m\rangle$ and $|m+n\rangle$ refer to the vibrational states with $m$ and $m+n$ number of vibrational quantum, respectively. The atomic ground and excited states are represented by $|g\rangle$ and $|e\rangle$, respectively. The states $|\psi_m^\pm\rangle$, $m=0,1,2,\ldots$, constitute the $(m+1)$th manifold of the excited dressed states. The corresponding eigenvalues are

$$\lambda_\pm = \left(m + \frac{n}{2}\right)\nu \pm \beta(m), \tag{19}$$

where $\beta(m)$ is the effective Rabi frequency of the nonlinear multiquantum JC-type interaction for the respective models. For a two-level atom

$$\beta(m) = \epsilon\sum_{k=0}^{m} f_k \frac{\sqrt{m!\,(m+n)!}}{(m-k)!}, \tag{20}$$

whereas for the three-level (effective two-level) atom

$$\beta(m) = \epsilon_r\sum_{k=0}^{m} F_k \frac{\sqrt{m!\,(m+n)!}}{(m-k)!}. \tag{21}$$

Since we are interested in the fluctuation dynamics around the Rabi oscillation we restrict our study to the initial deexcited state of the atom's electronic part. This is because the initial excited state adds to the fluctuations due to spontaneous emission. At $t=0$ the composite state of the system may be represented as

$$|\psi(0)\rangle = \sum_{m=0}^{\infty} C_m |m,g\rangle. \tag{22}$$

The constant $C_m$ is determined by the initial state of the vibrational motion. For the motion initially in the coherent state $|\alpha\rangle$,

$$C_m = \frac{\alpha^m}{\sqrt{m!}}\exp\left[-\frac{|\alpha|^2}{2}\right], \tag{23}$$

where $|\alpha|^2$ is the average number of vibrational excitation.

On expressing the initial state in terms of the eigenstates $|\psi_m^\pm\rangle$ of $H_I$ we get

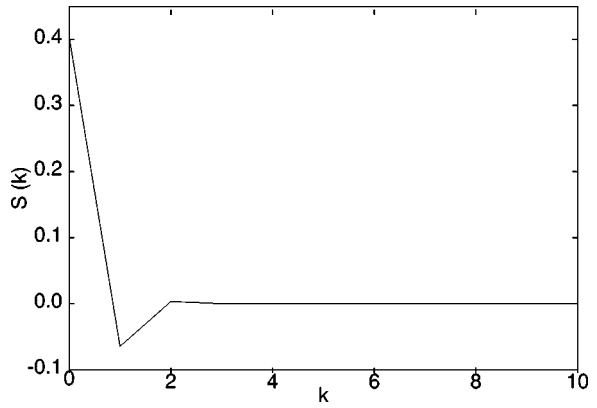


FIG. 2. $S(k)=f_k\sqrt{m!(m+n)!}/(m-k)!$ vs $k$ for the two-level atom model with $n=1$, $\xi=0.1$, $|\alpha|^2=10$, and $\phi_0=\pi/4$ taking $m=32$.

$$|\psi(0)\rangle = \frac{1}{\sqrt{2}}\sum_{m=0}^{\infty} C_m\{|\psi_{m-n}^{+}\rangle - |\psi_{m-n}^{-}\rangle\}. \tag{24}$$

The state at any later time $t$ is then given by

$$|\psi(t)\rangle = \sum_{m=0}^{\infty} C_m e^{-i(m-n/2)\nu t}\{\cos[\beta(m-n)t]|m,g\rangle - i\,\sin[\beta(m-n)t]|m-n,e\rangle\}. \tag{25}$$

Equation (25) describes the time evolution of the state function when the atom is initially prepared in the ground state and the atomic c.m. motion is coherent. This equation will be used in the following sections to determine the quantum averages of various system observables.

## V. DELAYED REVIVAL OF ATOMIC INVERSION

The time evolution of the average population in the state $|e\rangle$ is governed by

$$\langle\sigma_z(t)\rangle = \langle\psi(t)|\sigma_z|\psi(t)\rangle = -\frac{1}{2}\sum_{m=0}^{\infty}|C_m|^2\cos[2\beta(m-n)t]. \tag{26}$$

In the following sections we will discuss the collapse and revival pattern of atomic inversion for the model systems.

### A. Model I

It can be noticed from Eq. (3) that for $\xi<1$, $f_k$ decreases very rapidly as we increase the value of $k$. Hence the contribution to the Rabi frequency $\beta(m)$ comes mainly from $k=0$ term. As a typical example, in Fig. 2 we have plotted the function $S(k)=f_k\sqrt{m!(m+n)!}/(m-k)!$ as a function of $k$ for a particular value of $m$ with $\xi=0.1$, $|\alpha|^2=10$, $\phi_0=\pi/4$, and $n=1$.

The figure shows that the maximum of the function occurs at $k=0$ and also $S(k)$ reduces to zero within few $k$. The same is true for model II also.

Let us now consider the first term ($k=0$ term) of the series describing the Rabi frequency $\beta(m)$ given in Eq. (20),

$$\beta(m) = \epsilon f_0^{(n)}\frac{\sqrt{m!\,(m+n)!}}{m!} = g_n\sqrt{(m+1)(m+2)\cdots(m+n)}, \tag{27}$$

where $g_n=\epsilon f_0^{(n)}$ and $f_0^{(n)}$ is the value of $f_k$ for $k=0$ and $n$th vibrational level. With the above Rabi frequency the population inversion of Eq. (26) becomes

$$\langle\sigma_z\rangle = -\frac{1}{2}\sum_{m=0}^{\infty}|C_m|^2\cos\{2g_n t\sqrt{m(m-1)\cdots[m-(n-1)]}\}. \tag{28}$$

For $n=1$, Eq. (28) simplifies to

$$\langle\sigma_z\rangle = -\frac{1}{2}\sum_{m=0}^{\infty}|C_m|^2\cos(2g_1 t\sqrt{m}). \tag{29}$$

This expression for the atomic inversion is the same as that of the usual JC model of two-level atom interacting with single photon of a cavity mode.

For $n=2$, the population inversion of Eq. (28) reduces to

$$\langle\sigma_z\rangle = -\frac{1}{2}\sum_{m=0}^{\infty}|C_m|^2\cos[2g_2 t\sqrt{m(m-1)}]. \tag{30}$$

This result is the same as one would expect for the atomic inversion in the case of driven JC model or two-photon one-mode JC model [11–13]. The only difference is that, unlike the cavity modes, $m$ here represents the vibrational modes. Further, in the trapped atom case the coupling parameter $g_n$ is not a constant. It is a nonlinear function of LD parameter. Moreover, the coupling strength depends on the vibrational level.

The time evolution of population inversion shows usual collapse and revival pattern. In order to find the revival time we expand the function $\sqrt{m(m-1)\cdots[m-(n-1)]}$ about the average number of the vibrational quantum $m_0$. The first term in the Taylor series expansion of the above function, i.e., $\sqrt{m_0(m_0-1)\cdots[m_0-(n-1)]}$, leads to the usual Rabi oscillation. The second term or the first-order term in $(m-m_0)$ will determine the revivals. Thus revivals occur at times when two oscillations are in phase, or, when the coefficient of the term $(m-m_0)$ in the Taylor series expansion of the above function in the argument of cosine function in Eq. (28) satisfies the relation

$$g_n\left[\sqrt{\frac{m_0!}{(m_0-n)!}}\sum_{z=1}^{n}\frac{1}{[m_0-(z-1)]}\right]t_r^n = 2\pi l_n, \qquad l_n = 1,2,\ldots, \tag{31}$$

where $t_r^n$ is the revival time for the $n$th sideband transition process. Thus there will be series of revivals for $l_n=1$, $l_n=2$, and so on.

From Eq. (31) one can easily find the revival time for the first sideband transition ($n=1$) as

$$t_r^1 = 2\pi l_1 g_1^{-1} m_0^{1/2}, \quad g_1 = \epsilon f_0^{(1)}, \quad l_1 = 1,2,\ldots, \tag{32}$$

where $f_0^{(1)}$ is the value of $f_k$ for $k=0$ and $n=1$. Hence the ratio of the times for which the revival of the population inversion occurs first ($l_1=1, l_n=1$) in the $n$th ($n>1$) and first ($n=1$) sideband transition is

$$\frac{t_r^n}{t_r^1} = \frac{n!}{\xi^{n-1}} \frac{1}{m_0} \sqrt{\frac{(m_0-n)!}{(m_0-1)!}} \left[ \sum_{z=1}^{n} \frac{1}{[m_0-(z-1)]} \right]^{-1}. \tag{33}$$

In deriving the above form we have made use of Eq. (3) and adjusted the equilibrium position of the atom with respect to the node or the antinode of the standing wave so that the phase part of $f_k$ is unity in the respective cases. Equation (33) shows that for a particular value of $\xi$ and $m_0$ the time of occurrence of the first revival increases with the increase in $n$, the sideband index responsible for atomic transition. Also for a particular sideband transition the ratio increases with the decrease in $\xi$.

In order to examine the exact dependence of the vibrational quantum number on the revival time ratio, in the following we analyze the cases of second ($n=2$) and first ($n=1$) red-sideband transitions. The revival time for the second sideband transition ($n=2$), obtained from Eq. (31), reads as

$$t_r^2 = 2\pi l_2 g_2^{-1} \frac{\sqrt{m_0(m_0-1)}}{(2m_0-1)}. \tag{34}$$

Now dividing Eq. (34) by Eq. (32) we get the ratio of the times for which the population inversion revives first for the second and first sideband processes. So

$$\frac{t_r^2}{t_r^1} = \frac{g_1\sqrt{m_0-1}}{g_2(2m_0-1)} = \frac{2\sqrt{m_0-1}}{\xi(2m_0-1)}. \tag{35}$$

For $m_0 \gg 1$, the ratio reduces to

$$\frac{t_r^2}{t_r^1} = \frac{1}{\xi\sqrt{m_0}}. \tag{36}$$

Now if the right-hand side of Eq. (36) is greater than unity, i.e., the product $\xi\sqrt{m_0}$ is less than unity then $t_r^2$ will be greater than $t_r^1$, or the first revival in the second sideband transition will occur at a later time than the first revival in the first sideband transition. For a particular sideband transition process we have two controlling parameters to observe the delayed revival. They are (i) the LD parameter $\xi$ and (ii) the average quantum number of the initial coherent vibration, $m_0=|\alpha|^2$. Thus the time evolution of the inversion may exhibit delayed-revival phenomena even in the LD regime if the initial number of the vibrational quantum is bounded by the relation $m_0 < 1/\xi^2$.

The physical reason behind the $\xi$, $n$, and $|\alpha|^2$ dependence of the revival time is the following. The collapse and revival is the result of the interference between different Rabi frequencies corresponding to different values of vibrational quantum number in their distribution, which is coherent initially. The structure of the revivals thus depends on probability distribution $|C_m|^2$ (hence $|\alpha|^2$) of the vibrational states and the vibrational quantum number dependent Rabi frequency $\beta(m)$. The $\xi$ and $n$ dependence of the revival time comes from oscillation period $\beta(m)$ which is a function of both LD parameter and vibrational level through $f_k$ or $F_k$ as the case may be. In fact, delayed revival for any $n$th trap state as compared to the first state is expected for any value of $\xi$ provided the number of vibrational quantum present in the mode can cause $n$ sideband transition of the trapped states. When $\xi$ is large the motional states are very close together and absorption and emission of a photon will always cause some change in the motional states of the atom. On the other hand when $\xi$ is small then the trap states are well spaced and many photons need be absorbed or emitted before the atom changes the vibrational level. This paper, to the best our knowledge, is the first one to study the delayed-revival phenomena in two-level and three-level atoms undergoing quantum oscillations in a harmonic trap and interacting with classical em field.

For further illustration we take the example of $m_0=10$. The value of the ratio $t_r^2/t_r^1$, as calculated from Eq. (36), is $\approx 316$ and 3 for $\xi=0.001$ and $\xi=0.1$, respectively. Thus the first revival in the second sideband process occurs at 316 and three times the first revival time for first sideband process for the above two cases.

### B. Model II

In Sec. III we have shown that three-level trapped atom interacting with two em fields can be reduced to effective two-level system by eliminating the second excited state. We have also shown that except the effective coupling strength the effective two-level atom Hamiltonian (14) is the same as the two-level atom Hamiltonian (4) presented in Sec. II. Hence, the general expression for the revival time (31) derived for the two-level atom case holds for the three-level atom case also except the coupling constant $g$. Following Eqs. (32) and (34) we may express the first revival time of the atomic inversion for the first and the second sideband transition cases as

$$t_r^1 = \frac{2\pi\sqrt{m_0}}{g_1'} \tag{37}$$

and

$$t_r^2 = \frac{2\pi\sqrt{m_0(m_0-1)}}{g_2'(2m_0-1)}, \tag{38}$$

respectively, with

$$g_1' = \epsilon_r F_0^{(1)} = -\epsilon_r [e^{-\xi_+^2/2}\xi_+ \sin\phi_+ - e^{-\xi_-^2/2}\xi_- \sin\phi_-] \tag{39}$$

and

$$g_2' = \epsilon_r F_0^{(2)} = -(\epsilon_r/2)[e^{-\xi_+^2/2}\xi_+^2 \cos\phi_+ - e^{-\xi_-^2/2}\xi_-^2 \cos\phi_-]. \tag{40}$$

Thus for $m_0 \gg 1$, the ratio of the revival times is

$$\frac{t_r^2}{t_r^1}=\frac{g_1'}{2g_2'\sqrt{m_0}}=\frac{1}{\sqrt{m_0}}\frac{e^{-\xi_+^2/2}\xi_+\sin\,\phi_+-e^{-\xi_-^2/2}\xi_-\sin\,\phi_-}{e^{-\xi_+^2/2}\xi_+^2\cos\,\phi_+-e^{-\xi_-^2/2}\xi_-^2\cos\,\phi_-}. \tag{41}$$

If we take $\phi_+=\phi_-=\pi/2$ for $n=1$ and $\phi_+=\phi_-=0$ for $n=2$, then the ratio becomes

$$\frac{t_r^2}{t_r^1}=\frac{1}{\sqrt{m_0}}\frac{e^{-\xi_+^2/2}\xi_+-e^{-\xi_-^2/2}\xi_-}{e^{-\xi_+^2/2}\xi_+^2-e^{-\xi_-^2/2}\xi_-^2}, \tag{42}$$

which is a complicated function of $\xi_1$ and $\xi_2$. For delayed revival to occur for $n=2$ the right-hand side of the above expression has to be greater than unity. Dividing the numerator and the denominator of the right-hand side of Eq. (42) by $\xi_+^2\exp(-\xi_+^2/2)$ we may rewrite the ratio of the two revival times as

$$\begin{aligned}\frac{t_r^2}{t_r^1}&=\frac{1}{\xi_+\sqrt{m_0}}\frac{1-e^{(\xi_+^2-\xi_-^2)/2}(\xi_-/\xi_+)}{1-e^{(\xi_+^2-\xi_-^2)/2}(\xi_-^2/\xi_+^2)}\\&=\frac{1}{\xi_+\sqrt{m_0}}\frac{1-e^{2\xi_1\xi_2}(1-\xi_2/\xi_1)/(1+\xi_2/\xi_1)}{1-e^{2\xi_1\xi_2}(1-\xi_2/\xi_1)^2/(1+\xi_2/\xi_1)^2}.\end{aligned} \tag{43}$$

As it is not very obvious from the general expression of the time ratio given by Eq. (43) that revivals for $n=2$ are delayed, we examine the same in some special cases.

(i) $\xi_1\gg\xi_2$, so $\xi_2/\xi_1\ll 1$, Eq. (43) approximates to

$$\frac{t_r^2}{t_r^1}\approx\frac{1}{\xi_+\sqrt{m_0}}, \tag{44}$$

which is same as Eq. (36), obtained for the two-level atom model, except that $\xi$ is replaced by $\xi_+\approx\xi_1$.

(ii) $\xi_1=\xi_2$, the expression for the time ratio of Eq. (43) simplifies to

$$\frac{t_r^2}{t_r^1}=\frac{1}{2\xi_1\sqrt{m_0}}. \tag{45}$$

This is again same as Eq. (36) with $\xi$ replaced by $2\xi_1$.

(iii) $\xi_1\ll\xi_2$, so $\xi_2/\xi_1\gg 1$, it can be shown that

$$\frac{t_r^2}{t_r^1}\approx\frac{1}{\xi_+\sqrt{m_0}}\frac{1+e^{2\xi_1\xi_2}}{1-e^{2\xi_1\xi_2}}. \tag{46}$$

If the value of $\xi_1$ and $\xi_2$ are such that the product $2\xi_1\xi_2\ll 1$ then time ratio can be further simplified to

$$\frac{t_r^2}{t_r^1}\approx\frac{1}{\xi_+\xi_1\xi_2\sqrt{m_0}}, \tag{47}$$

with a minus sign which could be removed by a proper choice of the equilibrium position of the atom. For the same values of $\xi_1$, $\xi_2$, and $m_0$ this case offers larger revival time in $n=2$ process than case (i) and case (ii).

We have therefore proved that under suitable values for the parameters $\xi_1$, $\xi_2$, and $m_0$ large time-scale revivals do occur in three-level trapped atom also. In fact the three-level atom does not play any extra role in the generation of delayed-revival pattern as long as it is picturized as effective two-level system whose dynamics is no different from actual two-level atom system.

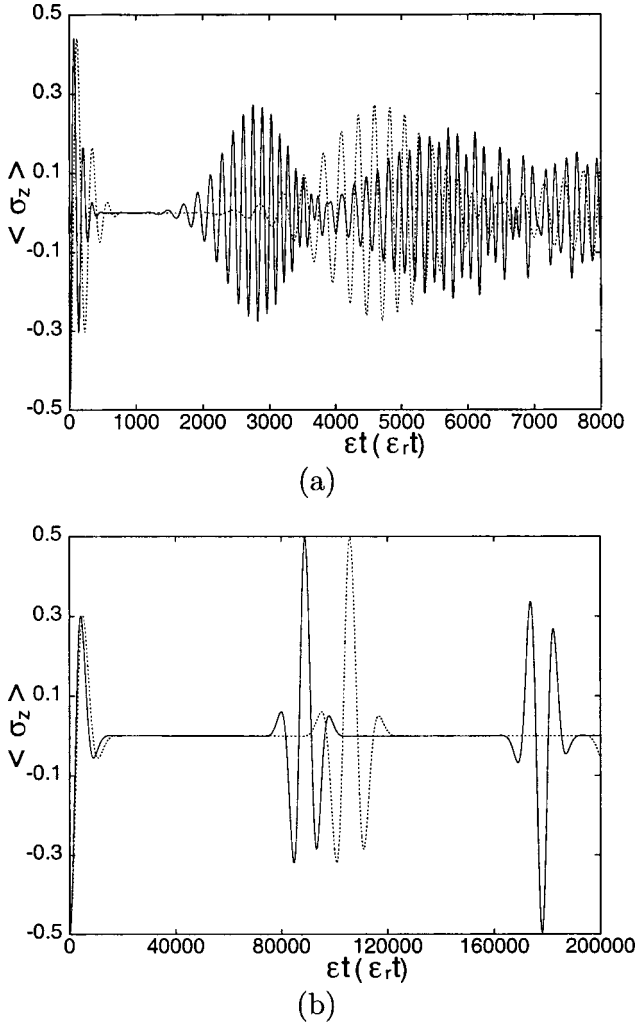


FIG. 3. The atomic inversion $\langle\sigma_z\rangle$ plotted as a function of $\epsilon t$ (two-level atom) in the solid curve with $\xi=0.01$, $\phi_0=\pi/4$, and $\epsilon_r t$ (effective two-level atom) in the dashed curve with $\xi_1=0.007$, $\xi_2=0.003$, $\phi_1=\pi/4$, $\phi_2=0$, $|\alpha|^2=10$ for (a) $n=1$, (b) $n=2$.

In Fig. 3 we have plotted the atomic inversion given in Eq. (26) as a function of scaled time $\epsilon t$ (solid curve) and $\epsilon_r t$ (dashed curve) with Fig. 3(a) and 3(b) representing the cases of $n=1$ and $n=2$, respectively. The solid curves in both the figures refer to the case of two-level atom with $\xi=0.01$, $m_0=|\alpha|^2=10$, and $\phi_0=\pi/4$ whereas the dashed curves are plotted for the effective two-level model with $\xi_1=0.007$, $\xi_2=0.003$, $\phi_1=\pi/4$, and $\phi_2=0$. The first revival in Fig. 3(a) occurs at $\epsilon t\approx 2808$ in the solid curve and $\epsilon_r t\approx 4683$ in the dashed curve. The positions are matching with those predicted analytically in Eqs. (32) and (37). Note from the curves of Fig. 3(b) that the first revival occurs at $\epsilon t\approx 88\,425$ (in solid curve) and $\epsilon_r t\approx 105\,642$ (in dashed curve). Thus the revival in Fig. 3(b) seems to be occurring at much greater value of $\epsilon t(\epsilon_r t)$ than in Fig. 3(a).

The physical reason behind this delayed revival in Fig. 3(b) corresponding to $n=2$ as compared to Fig. 3(a) corre-

sponding to $n=1$ can be explained by looking into the expressions for the effective Rabi frequency and $f_k$ given by Eqs. (20) and (3), respectively. These two equations suggest that for the same value of $\xi$ and $m$,

$$\beta(m)|_{n=2} \ll \beta(m)|_{n=1}. \tag{48}$$

The revival time $t_r$ is estimated as the time when two neighboring terms in Eq. (26) for $m=m_0$ and $m=m_0+1$ differ in phase by a factor of $2\pi$ or in other words $t_r$ satisfies the relation $\{2\beta(m_0+1)-2\beta(m_0)\}t_r=2\pi$. Since the product of $\beta(m)$ and $t_r$ is constant, hence it proves that

$$t_r|_{n=2} \gg t_r|_{n=1}. \tag{49}$$

In the similar way, it can be easily shown that as $n$ increases the revival time $t_r$ increases at the cost of decreased value of Rabi frequency $\beta(m)$. The different frequency of oscillation makes the curves in Fig. 3(b) look different from those of Fig. 3(a).

Moreover, it can be noticed from Figs. 3(a) and 3(b) that the ratio of the first revival times is $t_r^2/t_r^1=88\,425/2808=31.4$ for model I (solid curve). This is close to the value predicted in Eq. (36) as for $\xi=0.01$ and $m_0=10$, $1/\xi\sqrt{m_0}=31.6$. The ratio of the revival times as observed from the dashed curves is $105\,642/4683=22.55$ which is close to $1/2\xi_1\sqrt{m_0}=22.58$. The overall collapse and revival pattern of the inversion dynamics of the effective two-level model is same as the two-level atom model.

## VI. DYNAMICS OF THE VIBRATIONAL MODE

The time evolution of the average number of the vibrational excitation is governed by

$$\langle N(t)\rangle = \langle a^\dagger(t)a(t)\rangle = \langle \psi(t)|a^\dagger a|\psi(t)\rangle = \sum_{m=0}^{\infty} |C_m|^2\{m - n\,\sin^2[\beta(m-n)t]\}. \tag{50}$$

In Fig. 4 we have plotted the average excitation number $\langle N\rangle$ as a function of scaled time from Eq. (50). Figure 4(a) and 4(b) refer to the cases of $n=1$ and $n=2$, respectively. The solid curves in both Figs. 4(a) and 4(b) are plotted for model I with $\xi=0.1$, $m_0=10$, and $\phi_0=\pi/4$ whereas the dashed curves refer to model II with $m_0=10$, $\xi_1=0.07$, $\xi_2=0.03$, $\phi_1=\pi/4$, and $\phi_2=0$. The curves show that the average excitation number exhibits the similar pattern of collapse and revival as seen in the atomic population inversion. The time evolution of the average vibrational quantum number and the average population inversion is such that the sum of two is a constant of motion, i.e., at any time

$$\langle N(t)\rangle + n\langle \sigma_z(t)\rangle = \text{const}. \tag{51}$$

Also for any $n$th sideband transition both the variables oscillate with frequency $2\beta(m-n)$. Comparing the plots of Figs. 3 and 4 one can easily note that the revival occurs at much earlier time in Fig. 4 than in Fig. 3 for both the first [the curves (a)] and second [curves (b)] sideband transition processes. This is expected as the values of LD parameters chosen for plotting the respective cases of Fig. 4 are more by one order of magnitude than those in Fig. 3. This supports our theoretical derivation of the revival time presented in Sec. V. The estimate for the ratio of revival times as derived in that section remains unaltered for the time evolution of vibrational excitation.

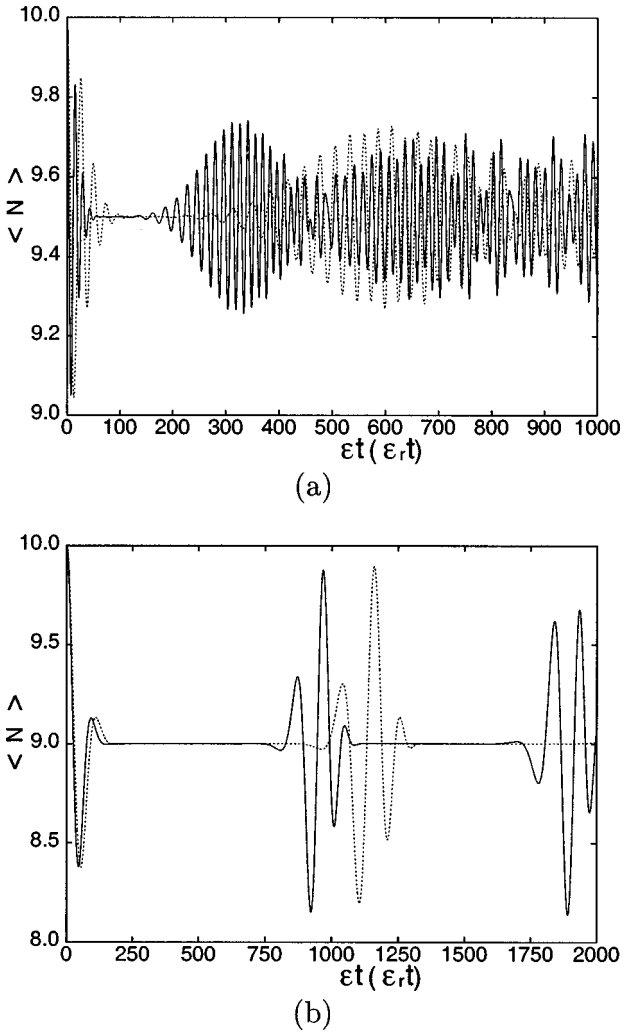


FIG. 4. The average number of motional quantum $\langle N\rangle$ plotted as a function of $\epsilon t$ in the solid curve with $\xi=0.1$, $\phi_0=\pi/4$, and $\epsilon_r t$ in the dashed curve with $\xi_1=0.07$, $\xi_2=0.03$, $\phi_1=\pi/4$, $\phi_2=0$, and $|\alpha|^2=10$ for (a) $n=1$, (b) $n=2$.

The qualitative difference between the curves for $n=1$ and $n=2$ of Fig. 4 is due to the difference in their oscillation frequency. As $n$ increases the vibrational-assisted Rabi frequency decreases thereby increasing the revival time. It can also be observed from the curves of Figs. 4(a) and 4(b) that the ratio $t_r^2/t_r^1$ is 3.15 for the solid curves and 2.25 for the dashed curves. These values are close to the analytical results given in Eqs. (36) and (47), respectively.

## VII. NONCLASSICAL STATES OF THE VIBRATIONAL MODE

In order to investigate the nonclassical properties of the vibrational quantum, which plays the same role as the pho-

tons of the cavity field in JC interaction, we examine the second-order coherence function of the motional state defined as [11]

$$\gamma^{(2)} = \frac{\langle a^{\dagger 2} a^2 \rangle}{\langle a^\dagger a \rangle^2}, \tag{52}$$

which in terms of normally ordered variance of the vibrational quantum number denoted by $\langle :\Delta N^2: \rangle$, with

$$\langle :\Delta N^2: \rangle = \langle a^{\dagger 2} a^2 \rangle - \langle a^\dagger a \rangle^2,$$

may be rewritten as

$$\gamma^{(2)} = 1 + \frac{\langle :\Delta N^2: \rangle}{\langle N \rangle^2}, \quad N = a^\dagger a. \tag{53}$$

The time evolution of $\langle a^\dagger a \rangle$ is given in Eq. (50). Using Eq. (25) it is trivial to find that the time evolution of $\langle a^{\dagger 2} a^2 \rangle$ is governed by

$$\langle a^{\dagger 2} a^2 \rangle = \sum_{m=0}^{\infty} |C_m|^2 \{ m(m-1) + (n^2 - 2mn + n) \times \sin^2[\beta(m-n)t] \}. \tag{54}$$

In Fig. 5 we present the behavior of the normally ordered variance $\langle :\Delta N^2: \rangle$ of motional quantum for $n=1$ in Fig. 5(a) and $n=2$ in Fig. 5(b), respectively. The solid curves of both the figures represent the case of two-level atom model with $\xi=0.1$, $m_0=5$, and $\phi_0=\pi/4$. The dashed curves show the variance for the effective two-level atom model plotted with $\xi_1=0.08$, $\xi_2=0.02$, $\phi_1=\pi/4$, $\phi_2=0$, and the same value of $m_0$.

From both the curves of Figs. 5(a) and 5(b) it is clear that at certain times on its evolution the motional quantum is generated with statistical fluctuations greater than that would be expected on the basis of Poissonian statistics, i.e., $\langle :\Delta N^2: \rangle > 0$. At those times the second-order coherence $\gamma^{(2)}$ is greater than unity and the motional quanta are said to be bunched. It is also observed that at some time intervals the motional quanta are generated with statistical fluctuations less than the coherent state value, i.e., $\langle :\Delta N^2: \rangle < 0$. In this situation the number distribution of motional modes is said to follow the sub-Poissonian statistics. This latter phenomenon is similar to the antibunching of the photons in cavity QED. At those time intervals where the motional states follow the sub-Poissonian statistics the second-order coherence $\gamma^{(2)}$ is less than unity thereby implying the generation of nonclassical states of the motional states.

Note that the time duration for which the variance is negative is more in $n=2$ [Fig. 5(b)] than in $n=1$ [Fig. 5(a)] case. The physical reason behind this generation of longer antibunched state ($\gamma^{(2)} < 1$) for $n=2$ process than $n=1$ is the following. Once the atom emits one vibrational quantum the second quantum cannot be emitted by the same atom until the atom is reexcited to its upper electronic state by the absorption of a motional quantum from the motional mode. This is done in a time determined by the vibrational-assisted Rabi frequency. The greater Rabi frequency of $n=1$ case

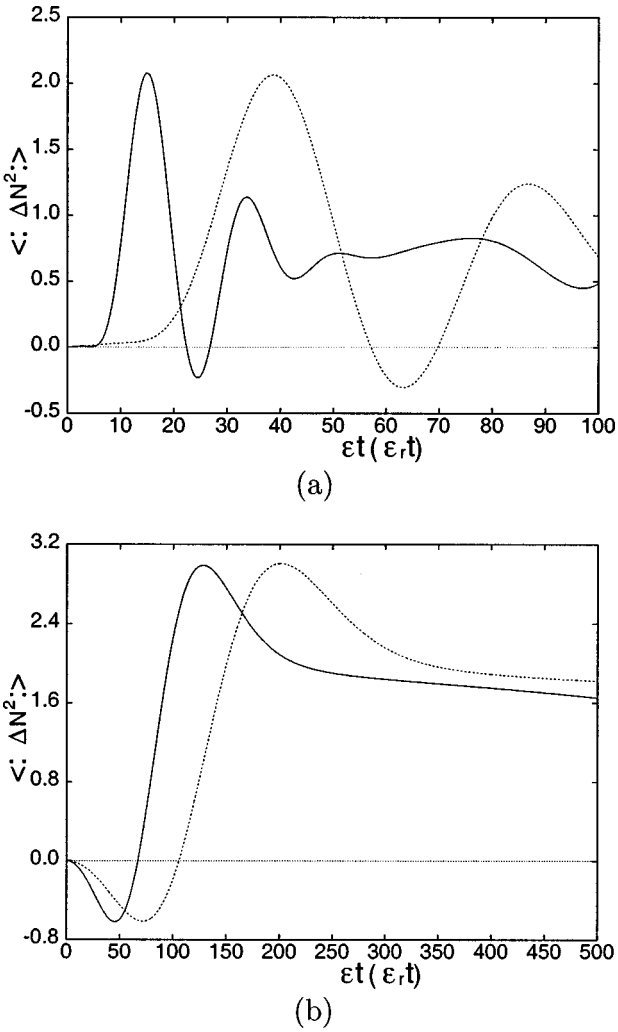


FIG. 5. The normally ordered variance of motional quantum $\langle :\Delta N^2: \rangle$ vs $\epsilon t$ (solid curves) with $\xi=0.1$, $\phi_0=\pi/4$, and $\epsilon_r t$ (dashed curve) with $\xi_1=0.08$, $\xi_2=0.02$, $\phi_1=\pi/4$, $\phi_2=0$, $|\alpha|^2=5$ for (a) $n=1$, (b) $n=2$.

permits the variance to be zero upto some time after which it starts deviating from coherent state. The smaller value of Rabi frequency for $n=2$ case maintains the antibunching for longer time.

The bunching and antibunching phenomena of the motional state are the result of the similar physical process that is responsible for the bunching and antibunching of the photons on interaction with two-level or three-level atoms in a high-$Q$ cavity. Moreover, the nonclassical behavior of the vibrational excitation exhibited in Fig. 5 is similar to those exhibited by the average photon numbers of the two modes of the cavity field (Raman coupled with three-level atom) as reported in Ref. [11]. The time behavior of the variance in the photon number of the first mode of the cavity field of that reference plotted for finite number of photons initially appears to be same as the time evolution of the normally ordered variance of the vibrational excitation shown in Fig. 5(a) referring to $n=1$. Further, the variance in the photon number of the second mode, with zero average number of photons initially, is similar to the normal order fluctuation of

the motional excitation plotted in Fig. 5(b) referring to $n=2$ case.

### VIII. SQUEEZED MOTIONAL STATES

Following Ref. [6] we consider the quadrature operator

$$x_\theta = ae^{i\theta} + a^\dagger e^{-i\theta}, \tag{55}$$

so that the position and the momentum of the atom's c.m. is directly proportional to $x_0$ and $x_{\pi/2}$, respectively. Accordingly the variances $(\Delta x_0)^2$ and $(\Delta x_{\pi/2})^2$ give the measure of the quantum noise associated with the atomic position and momentum. Those variances are related to the averages of the quadratic combinations of the creation and annihilation operators of the vibrational motion by the following relations:

$$(\Delta x_0)^2 = [1 + 2\ \mathrm{Re}\langle a^2\rangle + 2\langle a^\dagger a\rangle - 4\{\mathrm{Re}\langle a\rangle\}^2], \tag{56}$$

$$(\Delta x_{\pi/2})^2 = [1 - 2\ \mathrm{Re}\langle a^2\rangle + 2\langle a^\dagger a\rangle - 4\{\mathrm{Im}\langle a\rangle\}^2]. \tag{57}$$

The uncertainties in the observables $x_0$ and $x_{\pi/2}$ are constrained by Heisenberg uncertainty relation

$$(\Delta x_0)^2(\Delta x_{\pi/2})^2 \geqslant 1. \tag{58}$$

A coherent state of motion is the one for which the uncertainty product is minimum and the two quadratures have equal variance, $(\Delta x_0)^2=(\Delta x_{\pi/2})^2=1$. A quadrature component is said to be squeezed if the value of its variance is less than the value it has in the coherent state.

Assuming the vibrational motion to be initially in the coherent state we study the variances in the position and the momentum $(\Delta x_0)^2$ and $(\Delta x_{\pi/2})^2$ as a function of dimensionless time $\epsilon t$ for the atom initially in its ground state. The initial ground state does not contribute to the fluctuation due to spontaneous emission, hence it offers early onset to the quadrature squeezing. It is found that at certain time intervals either $(\Delta x_0)^2$ or $(\Delta x_{\pi/2})^2$ is less than 1, which is their corresponding coherent-state value. At those time intervals the position or the momentum exhibits squeezing. We find out numerically those time intervals where the position or the momentum of the c.m. of the atom is squeezed. In Figs. 6(a) and 6(b) we have illustrated the way to achieve the squeezing at earlier time by increasing the LD parameter. We consider the situation of the standing wave in the two-level atom model, when the center of mass of the atom coincides with the center of the trap, i.e., $\phi_0=0$. The figures show the time evolution of the variances in $x_0$ and $x_{\pi/2}$ for first red-sideband transition with $\nu=10\epsilon$, $m_0=8$. The solid and the dashed curves of Fig. 6(a) correspond to $(\Delta x_{\pi/2})^2$ and $(\Delta x_0)^2$, respectively, for $\xi=0.005$. Figure 6(b) represents the same but for $\xi=0.2$. It can be easily seen that the squeezing in momentum or position occurs at earlier times in Fig. 6(b) as compared to that in Fig. 6(a). So there is a decrease in the minimum time of occurrence of the squeezed states as we go for large recoiling of the atom as compared to the wavelength of the interacting field. If the recoil of the atom is considered to be much smaller than the wavelength of the interacting laser then the onset of the system to squeezing will be delayed.

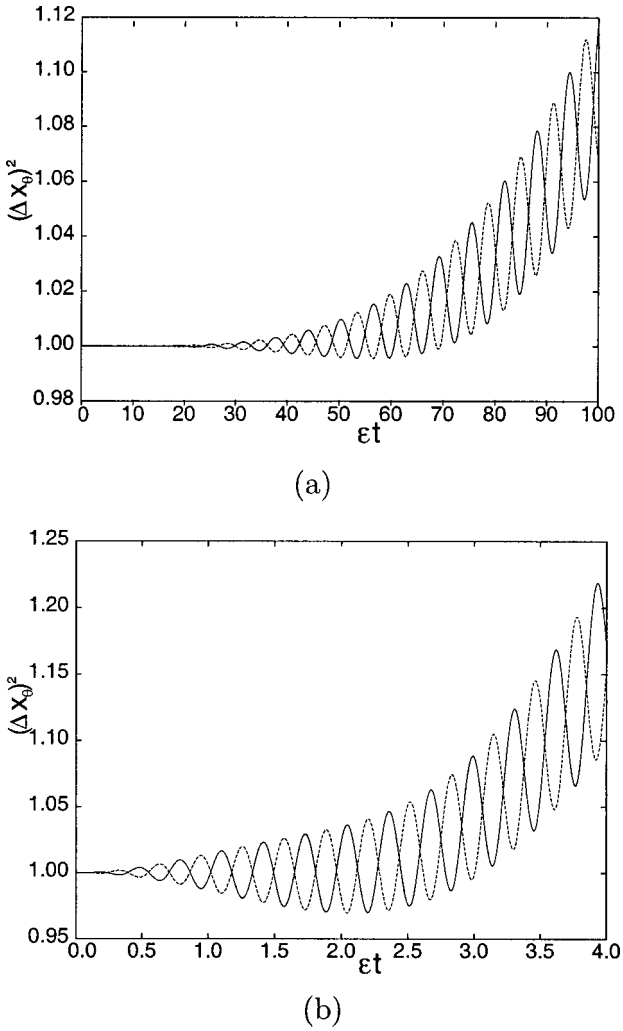


FIG. 6. The variance in momentum $(\Delta x_{\pi/2})^2$ (solid) and position $(\Delta x_0)^2$ (dashed) vs $\epsilon t$ for (a) $\xi=0.005$, (b) $\xi=0.2$ with $\nu=10\epsilon$, $|\alpha|^2=8$.

The $\xi$ dependence on the generation of the squeezed states is very normal, as for small LD parameter the spatial extension of the motional wave packet of the trapped atom is small compared with the wavelength of the driving laser. When the atom is weakly localized or $\xi$ is large then the interference of the atomic matter wave with the irradiating laser field leads to the nonlinear modification of the dynamics of the laser driven atom. When the spatial extension reaches a size of the order of magnitude of the laser wavelength then the atom-field interaction breaks down to the destructive interference between the motional wave and the laser wave. The squeezed states of the atomic motion are the outcome of such nonlinear effect.

To show how exactly the LD parameter changes the generation of the squeezed state we plot in Fig. 7 the minimum time for which $(\Delta x_0)^2$ is less than 1 as a function of $\xi$ for the same value of $\nu$ and $|\alpha|^2$ as used for Fig. 6. It is interesting to note that as the value of $\xi$ increases the corresponding time $(\epsilon t)_{min}$ does not decrease steadily rather it falls stepwise with a plateau at some very small $\xi$ domain. Though the overall behavior seems to be close to the function $\sim 1/\xi\sqrt{m_0}$, which

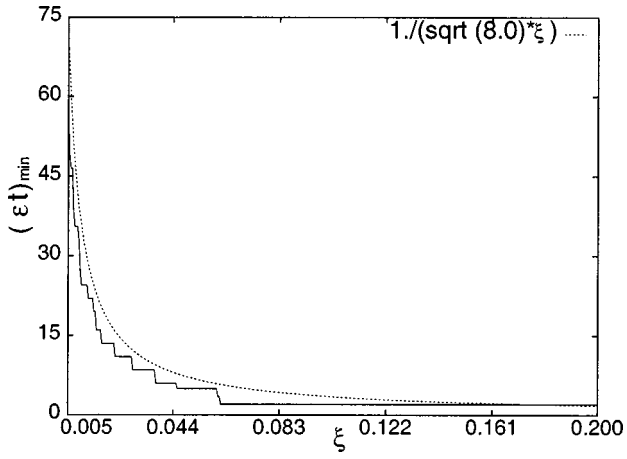


FIG. 7. The minimum time $(\epsilon t)_{min}$ for which $(\Delta x_0)^2<1$ vs $\xi$ for $\nu=10\epsilon$, $|\alpha|^2=8$.

is plotted as a function of $\xi$ in the dashed curve of Fig. 7, but the reason behind the stepwise fall is not very clear.

## IX. CONCLUSION

We have studied the dynamics of the two-level and three-level atom in a harmonic trap paying special attention to the observation of the large time-scale revivals termed as delayed revivals. We conclude that as the sideband index responsible for atomic transition increases the revival in the system observables occur at longer times. Also we have shown that the LD parameter and average number of initial vibrational excitation are the two parameters that largely influence the existence of delayed revival. It is shown that the time duration for which the motional quantum is antibunched is more for second sideband transition process than the first sideband transition process. The minimum time for which the early onset to the quadrature squeezing occurs is shown to be decreasing with the increase in the LD parameter.

## APPENDIX

In this appendix we derive the effective two-level Hamiltonian [Eq. (8)] for the present three-level atom in $\Lambda$ configuration by adiabatic removal of the excited state.

The Heisenberg equations of motion for the atomic transition operators $\sigma_{gr}$ and $\sigma_{re}$ corresponding to the Hamiltonian (7) are

$$\dot{\sigma}_{gr} = -i[(E_r - E_g)\sigma_{gr} + \epsilon_1(\sigma_{gg} - \sigma_{rr})\sin(k_1R + \phi_1)e^{-i\omega_1 t} + \epsilon_2\sigma_{ge}\sin(k_2R + \phi_2)e^{-i\omega_2 t}], \tag{A1}$$

$$\dot{\sigma}_{re} = i[(E_r - E_e)\sigma_{re} + \epsilon_1\sigma_{ge}\sin(k_1R + \phi_1)e^{i\omega_1 t} - \epsilon_2(\sigma_{rr} - \sigma_{ee})\sin(k_2R + \phi_2)e^{i\omega_2 t}]. \tag{A2}$$

Here we introduce the slowly varying operators $\tilde{\sigma}_{gr}$, $\tilde{\sigma}_{re}$, $\tilde{\sigma}_{ge}$ for the atomic variables as

$$\sigma_{gr} = \tilde{\sigma}_{gr}\, e^{-i(\omega_1+q\nu)t}, \quad \sigma_{re} = \tilde{\sigma}_{re}\, e^{i(\omega_2-p\nu)t},$$

$$\sigma_{ge} = \sigma_{gr}\cdot\sigma_{re} = \tilde{\sigma}_{ge}\, e^{-i(\omega_l+n\nu)t} = \tilde{\sigma}_{ge}e^{-i\omega_0 t}, \tag{A3}$$

with $\tilde{\sigma}_{ge}=\tilde{\sigma}_{gr}\cdot\tilde{\sigma}_{re}$. Substituting Eq. (A3) in Eqs. (A1) and (A2) we get the equations of motion for the new variables as

$$\dot{\tilde{\sigma}}_{gr} = -i[\Delta\tilde{\sigma}_{gr} + \epsilon_1(\sigma_{gg} - \sigma_{rr})\sin(k_1R + \phi_1)e^{iq\nu t} + \epsilon_2\tilde{\sigma}_{ge}\sin(k_2R + \phi_2)e^{-ip\nu t}] \tag{A4}$$

and

$$\dot{\tilde{\sigma}}_{re} = i[\Delta\tilde{\sigma}_{re} + \epsilon_1\tilde{\sigma}_{ge}\sin(k_1R + \phi_1)e^{-iq\nu t} - \epsilon_2(\sigma_{rr} - \sigma_{ee})\sin(k_2R + \phi_2)e^{ip\nu t}]. \tag{A5}$$

For large detuning $(\Delta \gg \nu)$ the approximate solutions of Eqs. (A4) and (A5) are found to be

$$\tilde{\sigma}_{gr} = -\frac{\epsilon_1}{q\nu+\Delta}(\sigma_{gg} - \sigma_{rr})\sin(k_1R + \phi_1)e^{iq\nu t} + \frac{\epsilon_2}{p\nu-\Delta}\tilde{\sigma}_{ge}\sin(k_2R + \phi_2)e^{-ip\nu t}, \tag{A6}$$

$$\tilde{\sigma}_{re} = -\frac{\epsilon_1}{q\nu+\Delta}\tilde{\sigma}_{ge}\sin(k_1R + \phi_1)e^{-iq\nu t} - \frac{\epsilon_2}{p\nu-\Delta}(\sigma_{rr} - \sigma_{ee})\sin(k_2R + \phi_2)e^{ip\nu t}. \tag{A7}$$

The terms diagonal in atomic variables $\sigma_{ii}$, $i=g,e,r$, lead to stark shifts which we shall assume to be negligibly small. By dropping these terms from Eqs. (A6) and (A7) we get the simplified solutions

$$\tilde{\sigma}_{gr} = \frac{\epsilon_2}{p\nu-\Delta}\tilde{\sigma}_{ge}\sin(k_2R + \phi_2)e^{-ip\nu t} \approx -\frac{\epsilon_2}{\Delta}\tilde{\sigma}_{ge}\sin(k_2R + \phi_2)e^{-ip\nu t}, \tag{A8}$$

$$\tilde{\sigma}_{re} = -\frac{\epsilon_1}{q\nu+\Delta}\tilde{\sigma}_{ge}\sin(k_1R + \phi_1)e^{-iq\nu t} \approx -\frac{\epsilon_1}{\Delta}\tilde{\sigma}_{ge}\sin(k_1R + \phi_1)e^{-iq\nu t}. \tag{A9}$$

Using Eq. (A3) we find the solutions of the original variables as

$$\sigma_{gr} = -\frac{\epsilon_2}{\Delta}\tilde{\sigma}_{ge}\sin(k_2R + \phi_2)e^{-ip\nu t}\, e^{-i\omega_1 t}\, e^{-iq\nu t} = -\frac{\epsilon_2}{\Delta}\sin(k_2R + \phi_2)\sigma_{ge}\, e^{-in\nu t}e^{-i\omega_1 t}e^{i\omega_0 t} = -\frac{\epsilon_2}{\Delta}\sigma_{ge}\sin(k_2R + \phi_2)e^{-i\omega_2 t} \tag{A10}$$

and

$$\sigma_{re} = -\frac{\epsilon_1}{\Delta}\sigma_{ge}\sin(k_1R+\phi_1)e^{i\omega_1 t}. \tag{A11}$$

With the above expressions [Eqs. (A10) and (A11)] for the atomic operators the Hamiltonian (7) reduces to

$$H = E_g\sigma_{gg} + E_r\sigma_{rr} + E_e\sigma_{ee} + \nu a^\dagger a - \frac{2\epsilon_1\epsilon_2}{\Delta} \times(\sigma_- e^{i\omega_l t} + \sigma_+ e^{-i\omega_l t})\sin(k_1R+\phi_1)\sin(k_2R+\phi_2), \tag{A12}$$

where we have introduced the effective atomic raising and the lowering operators $\sigma_+ = \sigma_{eg}$ and $\sigma_- = \sigma_{ge}$ between the levels $|g\rangle$ and $|e\rangle$. Since the level $|r\rangle$ is assumed to be far-off resonance we can set the occupation in that level to zero, i.e., $\sigma_{rr}=0$. Also defining the atomic inversion operator $\sigma_z$ as

$$2\sigma_z = \sigma_{ee} - \sigma_{gg} \tag{A13}$$

and shifting the zero of the energy scale at $(E_g+E_e)/2$ the Hamiltonian (A12) assumes the form

$$H = \omega_0\sigma_z + \nu a^\dagger a - 2\epsilon_r(\sigma_- e^{i\omega_l t} + \sigma_+ e^{-i\omega_l t}) \times\sin(k_1R+\phi_1)\sin(k_2R+\phi_2), \tag{A14}$$

where $\epsilon_r = \epsilon_1\epsilon_2/\Delta$ refers to the effective coupling constant for the two-level representation of the three-level model system.

Recall that there was no direct coupling between the two levels $|g\rangle$ and $|e\rangle$ originally and hence the dipole transition between them was forbidden. The application of the laser has made the coupling in such a way that it induces the transition $|g\rangle \leftrightarrow |e\rangle$. These are the two levels between which the population transfer takes place. We have thus derived the effective two-level Hamiltonian for the trapped three-level atom undergoing quantized motion.

Now, the wave vectors of the laser beams $k_1$ and $k_2$ are related with their corresponding LD parameters $\xi_1$ and $\xi_2$ in the following manner:

$$k_1R = \xi_1(a+a^\dagger), \quad k_2R = \xi_2(a+a^\dagger), \tag{A15}$$

where

$$R = \frac{1}{\sqrt{2M\nu}}(a+a^\dagger) \tag{A16}$$

is the position operator of the c.m. of the vibrating atom of mass $M$.

Using Eq. (A15) we can express the "sine" products appearing in Eq. (A14) as

$$\sin(k_1R+\phi_1)\sin(k_2R+\phi_2) = -\tfrac{1}{4}[e^{i\xi_+(a+a^\dagger)}e^{i\phi_+} + e^{-i\xi_+(a+a^\dagger)}e^{-i\phi_+} - e^{i\xi_-(a+a^\dagger)} \times e^{i\phi_-} - e^{-i\xi_-(a+a^\dagger)}e^{-i\phi_-}], \tag{A17}$$

with

$$\xi_\pm = \xi_1 \pm \xi_2, \quad \phi_\pm = \phi_1 \pm \phi_2. \tag{A18}$$

On using Eq. (A17) the Hamiltonian (A14) may be rewritten as

$$H = \omega_0\sigma_z + \nu a^\dagger a + \frac{\epsilon_r}{2}(\sigma_- e^{i\omega_l t} + \sigma_+ e^{-i\omega_l t})\{e^{i\xi_+(a+a^\dagger)}\, e^{i\phi_+} + e^{-i\xi_+(a+a^\dagger)}\, e^{-i\phi_+} - e^{i\xi_-(a+a^\dagger)}\, e^{i\phi_-} - e^{-i\xi_-(a+a^\dagger)}e^{-i\phi_-}\}. \tag{A19}$$

In the interaction picture or in a frame rotating with frequency $\omega_l$ the Hamiltonian (A19) reduces to

$$H_I = n\nu\sigma_z + \nu a^\dagger a + \frac{\epsilon_r}{2}\{e^{i\xi_+(a+a^\dagger)}\, e^{i\phi_+} + e^{-i\xi_+(a+a^\dagger)}\, e^{-i\phi_+} - e^{i\xi_-(a+a^\dagger)}\, e^{i\phi_-} - e^{-i\xi_-(a+a^\dagger)}e^{-i\phi_-}\}\{\sigma_+ + \sigma_-\}.$$


[1] F. Diedrich, J. C. Bergqist, W. M. Itano, and D. J. Wineland, Phys. Rev. Lett. **62**, 403 (1989).

[2] D. J. Wineland, J. Dalibard, and C. Cohen-Tannoudji, J. Opt. Soc. Am. B **9**, 32 (1992).

[3] A. Aspect, E. Arimondo, R. Kaiser, N. Vansteenkiste, and C. Cohen-Tannoudji, Phys. Rev. Lett. **61**, 826 (1988); J. Opt. Soc. Am. B **6**, 2112 (1989).

[4] D. M. Meekhof, C. Monroe, B. E. King, W. M. Itano, and D. J. Wineland, Phys. Rev. Lett. **76**, 1796 (1996); D. Liebfried, D. M. Meekhof, B. E. King, C. Monroe, W. M. Itano, and D. J. Wineland, *ibid.* **77**, 4281 (1996); C. Monroe, D. M. Meekhof, B. E. King, and D. J. Wineland, Science **272**, 1131 (1996).

[5] W. Vogel and R. L. de Matos Filho, Phys. Rev. A **52**, 4214 (1995).

[6] S. Wallentowitz and W. Vogel, Phys. Rev. A **58**, 679 (1998).

[7] Aditi Ray and R. R. Puri, Opt. Commun. **165**, 207 (1999).

[8] S. M. Dutra, P. L. Knight, and H. Moya-Cessa, Phys. Rev. A **49**, 1993 (1994).

[9] H. Moya-Cess, A. Vidiella-Barranco, J. A. Roversi, Dagoberto S. Freitas, and S. M. Dutra, Phys. Rev. A **59**, 2518 (1999).

[10] Aditi Ray (unpublished).

[11] C. C. Gerry and J. H. Eberly, Phys. Rev. A **42**, 6805 (1990); C. C. Gerry, *ibid.* **37**, 2683 (1988); C. C. Gerry and P. J. Moyer, *ibid.* **38**, 5665 (1988).

[12] S.-C. Gou, Phys. Rev. A **40**, 5116 (1989).

[13] R. R. Puri and G. S. Agarwal, Phys. Rev. A **37**, 3879 (1988); R. R. Puri and R. K. Bullough, J. Opt. Soc. Am. B **5**, 2021 (1988).